

# Biomechanical sensing of *in vivo* magnetic nanoparticle hyperthermia treated melanoma tumor using magnetomotive optical coherence elastography

Pin-Chieh Huang<sup>1,2</sup>, Eric J. Chaney<sup>1</sup>, Edita Aksamitiene<sup>1</sup>, Ronit Barkalifa<sup>1</sup>, Darold R. Spillman, Jr.<sup>1</sup>, Bethany J. Bogan<sup>1</sup>, and Stephen A. Boppart<sup>1,2,3,4,5</sup>

<sup>1</sup>Beckman Institute for Advanced Science and Technology, University of Illinois at Urbana-Champaign, USA

<sup>2</sup>Department of Bioengineering, University of Illinois at Urbana-Champaign, USA

<sup>3</sup>Department of Electrical and Computer Engineering, University of Illinois at Urbana-Champaign, USA

<sup>4</sup>Carle Illinois College of Medicine, University of Illinois at Urbana-Champaign, USA

<sup>5</sup>Cancer Center at Illinois, University of Illinois at Urbana-Champaign, USA

**Table S1. Stiffness changes after magnetic nanoparticle hyperthermia (MH) treatments**

Case	Local cellularity (%)	N <sup>†</sup>	$\Delta T_{\text{Max}}$ (°C)		$f_0^2$ change (%)		Statistical significance		
			After D1	After D2	After D1	After D2	B/D1	B/D2	D1/D2
0 kA/m (Control)		3	-2.55±0.67	-1.73±0.21	-6.0±10.3 (n = 46)	-13.3±22.1 (n = 53)	NS	NS	NS
61.2 kA/m, 5 min/dose	67.6±16.1 (Low)	4	9.98±3.40	9.30±1.82	-37.4±22.0 (n = 77)	-36.8±17.5 (n = 56) <sup>§</sup>	*****	*****	*****
	98.7±1.9 (High)	3	5.75±4.45 <sup>‡</sup>	8.50±3.68 <sup>‡</sup>	39.8±32.1 (n = 62)	48.5±66.7 (n = 43)	*****	***	NS
61.2 kA/m, 9 min/dose	79.7 (Low)	1	8.3		-24.6±9.1 (n = 18)		****		
	86.7 (High)	1	14.9		14.6±16.8 (n = 14)		NS		

**Abbreviations:** *MNPs*, magnetic nanoparticles; MM-OCE, magnetomotive optical coherence elastography; *N*, number of tumor samples; *n*, number of MM-OCE measurements; *B*, before treatment; *D1*, 1<sup>st</sup> MH dose treatment, *D2*, 2<sup>nd</sup> MH dose treatment. Statistical significance/insignificance are denoted with asterisks and hyphens, respectively. \*\*\*\*\*, \*\*\*\*, and \*\*\* denote a *p*-value less than 10<sup>-5</sup>, 10<sup>-4</sup>, and 10<sup>-3</sup>; “NS” denotes *p*-value > 0.01.

<sup>†</sup>Two samples are excluded from analysis – one without successful delivery of MNPs to the tumor core; the other with MNPs located in a highly heterogeneous tumor microenvironment (**Figure S2**).

<sup>‡</sup>Temperature measurement performed only on 2 out of 3 mice.

<sup>§</sup>Only 3 out of 4 mice were MH-treated for the 2<sup>nd</sup> time.

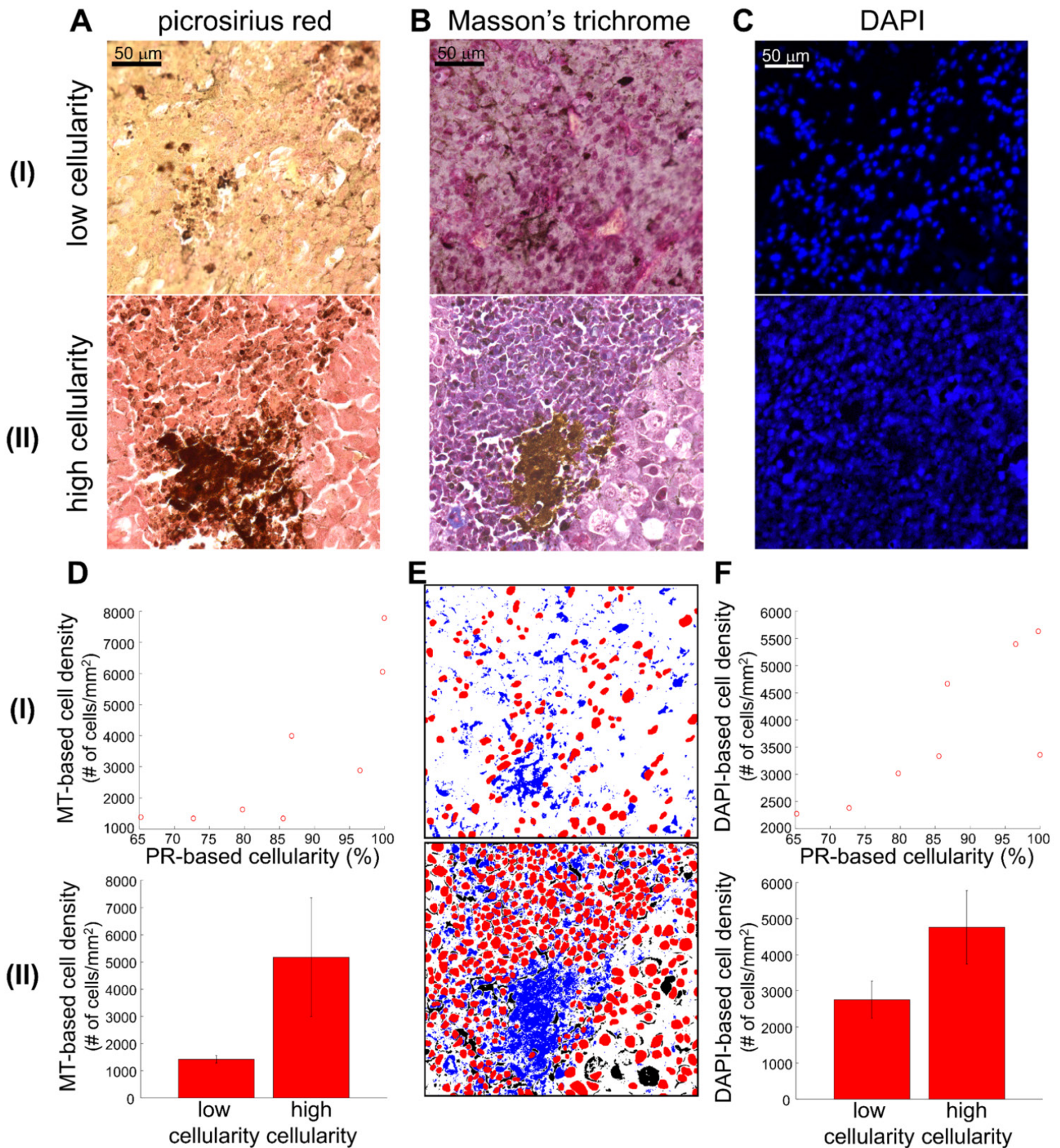


**Figure S1. Correlation between picosirius red (PR) color-based cellularity metrics and cell density (nuclei count per unit area) quantified based on Masson's trichrome (MT) and DAPI.** A-C. Representative images of low **(I)** and high **(II)** cellularity tumor sections stained with PR **(A)**, MT **(B)**, and DAPI **(C)**. **D**. PR-based cellularity correlates well with the cell density quantified based on MT histology (Pearson's  $r = 0.789$ ) **(I)**. The cell density of the high cellularity group ( $5.2 \pm 1.0 \times 10^3$  counts/mm<sup>2</sup>) was higher than that of the low cellularity group ( $1.4 \pm 0.1 \times 10^3$  counts/mm<sup>2</sup>) (two-sample t-test  $p = 0.014$ ) **(II)**. The nuclei were stained as dark purple in MT histology, **B (I, II)**, whose representative nucleus (*red*) and MNP (*blue*) segmentation was shown in **E (I, II)**, respectively. **F**. PR-based cellularity also correlates well with cell density quantified based on DAPI histology (Pearson's  $r = 0.786$ ) **(I)**. The cell density of the high cellularity group ( $4.8 \pm 1.0 \times 10^3$  counts/mm<sup>2</sup>) was higher than that of the low cellularity group ( $2.8 \pm 0.5 \times 10^3$  counts/mm<sup>2</sup>) (two-sample t-test  $p = 0.013$ ) **(II)**. The correlation analyses **(D, F)** were conducted on 8 AMF-treated tumors (11 in total, excluding one that showed absence of MNPs at tumor core, one that had MNPs trapped in a highly heterogeneous environment, **Figure S2**, and one severely necrotic tumor with limited histological sections, **Figure 2B**).



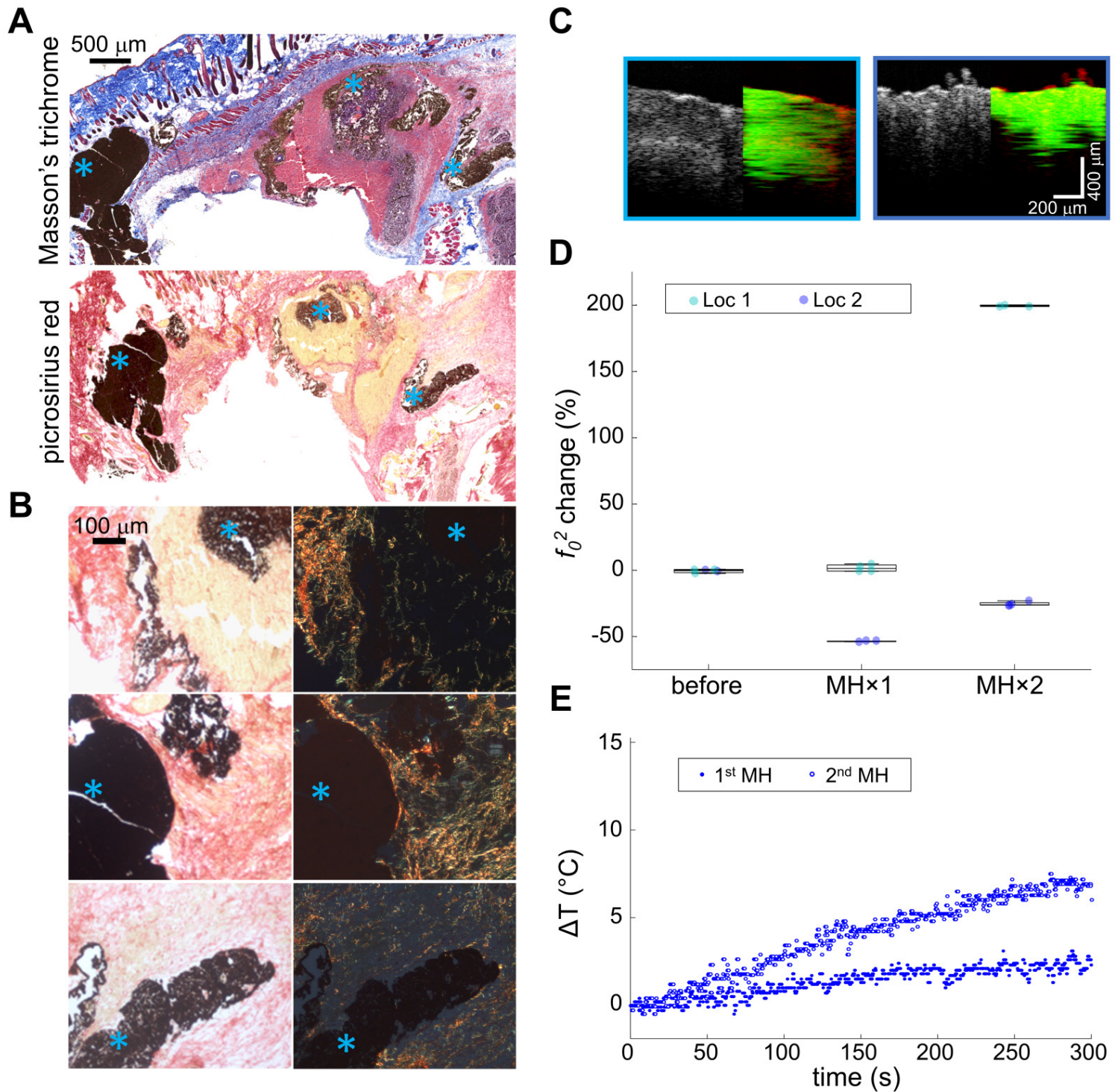


**Figure S2. Results from an MNP-injected melanoma tumor with MNPs present both at the tumor center and in the epidermis.** **A.** Images of Masson's trichrome (MT, *upper panel*) and picrosirius red (PR, *bottom panel*)-stained slides visualize the complex environment around the MNPs (*blue asterisks*) with either high or low local cellularity at the tumor site or immediately adjacent to collagen structures. **B.** Enlarged area from the PR-stained slide in **(A)** imaged with both brightfield (*left panel*) and polarized (*right panel*) light. Blue asterisks indicate MNPs. **C.** Optical coherence tomography (OCT, grey-scale) and the corresponding magnetomotive optical coherence tomography (MM-OCT, green and red) images obtained from two representative locations (Loc), where significant MM-OCT signals were observed at both sites, but **D.** the corresponding magnetomotive optical coherence elastography (MM-OCE) results exhibited noticeable differences, potentially suggesting sensitivity of MM-OCE to the local tumor environment near MNPs. **E.** The low rise of temperature after magnetic hyperthermia (MH) treatments.